Positron-induced dissociation of organic molecules

Jun Xu, Lester D. Hulett, Jr., T. A. Lewis, David L. Donohue, Scott A. McLuckey, and Gary L. Glish*
Oak Ridge National Laboratory, P.O. 2008, MS 6142, Oak Ridge, Tennessee 37831-6142
(Received 20 July 1992)

We have measured positron-ionization time-of-flight mass spectra of butylbenzene, decane, tetraethylsilane, and other organic molecules as a function of the positron kinetic energy. Our data show that fragment ions are produced at onset energies above the positronium- (Ps) formation threshold, while the molecular ions are formed starting at the Ps threshold. The onset energies have been found to depend strongly on the nature of the fragment and to be equal to the dissociation energy of the fragmentation reaction. Decreases in the molecular-ion populations in the mass spectra were observed to be accompanied by increases in fragment-ion populations. A two-step process, stripping followed by unimolecular dissociation, is proposed to be responsible for the production of the fragment ions. The degree of dissociation can be controlled by selecting the positron incident energy.

PACS number(s): 34.80.Dp, 36.10.Dr, 35.20.Gs, 78.70.Bj

I. INTRODUCTION

Studies of the dissociative ionization of molecules, using mass-spectrometry techniques, are useful in understanding the excitation of the internal energy and energy flow processes. Many different methods have been used to ionize molecules and/or impart energy to ions, such as photoionization dissociation [1,2], collision-induced dissociation [3], charge exchange [4], and electron-induced dissociation [5]. Observations of positron interactions with molecules may offer yet another method for studying the energy-transfer processes which lead to dissociation. Several theoretical [6] and experimental [7–9] treatments of positron ionization of molecules have recently been published which suggest that positron-ionization studies may provide additional insight.

The ionization processes of positrons and electrons in the low-energy range (0–50 eV) are significantly different. For electrons, positive ions are produced by the "knock-off process," whereby the electron passes close to the molecule and one or more electrons of the molecule are removed by the rapidly changing Coulombic field of the incoming electron to exceed the ionization potential of the molecule. For high-energy positrons (>70 eV) the cross sections are about the same as those of electrons [10], and the ion fragmentation patterns are quite similar [8], suggesting that the attractive force between the positron and the electrons imparts the same type of excitation to the molecule as that of the repulsive force imposed by electron impact. In addition to the high-energy process, there appear to be at least three additional mechanisms by which positive ions are produced by positron interactions with neutral molecules: (1) positronium formation, (2) electron pickoff, (3) positron attachment. Ionization by positronium formation occurs when the positron extracts an electron from the molecule and binds it to itself. The kinetic energy of the positron can be less than the binding energy of the molecule by as much as 6.8 eV, which is the magnitude of the positronium binding energy. Electron pickoff occurs when a positron passes by a molecule at a speed sufficiently slow to allow a large degree of overlap between the wave function of the positron and that of the bound electrons. Electron pickoff is often referred to as "in-flight" positron annihilation. Positron attachment is believed to occur by a process similar to that of electron attachment [11], whereby the incoming particle polarizes the molecule and becomes trapped in the resulting potential well. Positron attachment has been discussed theoretically by Schrader [6], and suggested experimentally by Surko and co-workers [12]. Typical organic molecules have ionization potentials in the range of 8–10 eV. Ionization by positronium formation therefore occurs at thresholds of 1.2–3.2 eV. The pickoff and attachment mechanisms occur at energies below the positronium-ionization threshold. In this paper we will discuss mainly the fragmentation processes that occur in the Ps-formation energy range.

In this work we studied the energy dependence of positron-induced dissociation of butylbenzene, decane, tetraethylsilane, benzene, hexene, octane, and dodecane. Our data show that fragment ions are produced at onset energies above the positronium- (Ps) formation threshold, while the molecular ions are formed starting at the Ps threshold. The onset energies have been found to strongly depend on the nature of the arrangement and to be equal to the enthalpy changes of the fragmentation reactions. The yields of molecular ions were seen to reach maxima for positron kinetic energies of 1–2 eV above the Ps thresholds; for positron energies beyond the maxima the yields of fragmentation ions increased and the yields of molecular ions decrease. A two-step process is proposed to be responsible for the production of the fragment ions. Our results indicate that the degree of dissociation can be controlled by selecting positron incident energy.

II. EXPERIMENTAL SETUP

Experimental setup, as schematically shown in Fig. 1, consists of the positron beamline, installed at the Oak

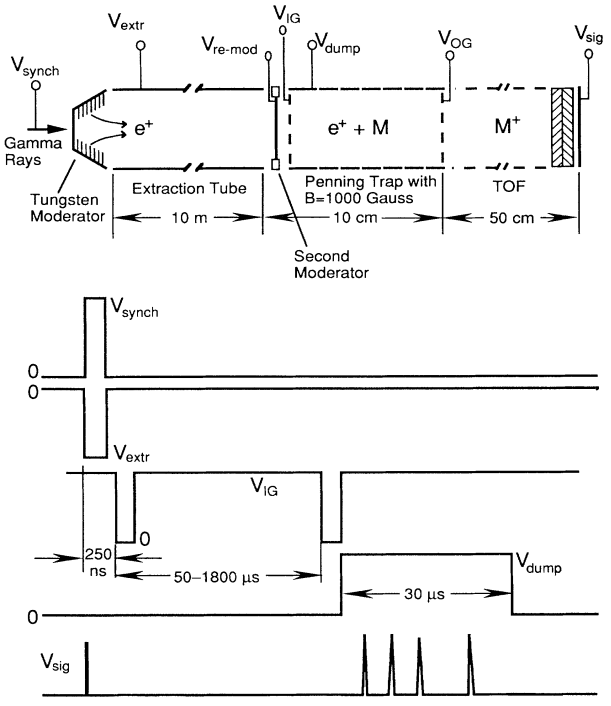

FIG. 1. Schematic diagram of the experimental setup, which includes the primary moderator, the extraction tube, the second moderator, the Penning trap, the quadratic-potential time-of-flight spectrometer, and microchannel-plate detector. IG denotes the input grid and OG denotes the output grid. The lower part of the diagram is the pulse sequence.

Ridge Electron Linear Accelerator (ORELA), and an ionization Penning trap jointly equipped with a quadratic-potential time-of-flight spectrometer (QP-TOF). The ORELA positron facility delivers 4-keV positrons to the mass spectrometer in 20–30-nsec pulses at repetition rates of 400–800 Hz. The experimental setup is operated by a pulse sequence that is synchronized to the ORELA delivery. The overall pulse sequence, also shown in Fig. 1, is as follows. (1) A start pulse from the ORELA (V_{synch}) initiates the sequence. (2) As positrons emerge from the tungsten moderator, a -4-kV pulse (V_{extr}) is applied to the extraction tube to accelerate the positrons out of the target room. (3) After about 250-nsec delay to allow the positrons to travel the 10-m distance to the second moderator, the input grid of the Penning trap is pulsed to ground potential ($V_{I/G}$) to allow the remoderated positrons to enter. The remoderated positrons are at low energy and require several nsec to travel to the output grid of the Penning trap. The positive potential of the input grid is restored before the reflected positrons can escape. A 1000-G magnetic field is applied longitudinally to the Penning trap, and the combined electrostatic and magnetic fields allow the positrons and resulting ions to be retained for periods of 1800 μs or longer. (4) At the end of the Penning trap retention period, the input grid is pulsed to ground potential for 1 μsec to allow residual positrons to escape the trap so that they will not generate excessive background in the mass spectra. (5) Following the positron-release pulse, the Penning trap and its adjoining flight path are pulled to positive potentials (V_{dump}) to expel the ions for time-of-flight mass measurements. (6) Ion signal pulses (V_{sig}) received by the microchannel plate detector serve as the stop of the pulse sequence.

Further details for the positron beam line and the Penning trap mass spectrometer are given in Refs. [13,14]. The ORELA produces a pulsed electron beam (pulse width: 10–20 ns; beam energy: 150 MeV; repetition rate: 800 Hz; power: 10 kW). The electron beam bombards a tantalum target and produces intense γ rays. γ photons that are less than 10 MeV are forward scattered beyond the tantalum target and are captured by an array of tungsten plates that converts them to electron-positron pairs. The tungsten plates have been annealed in such a manner that they also serve as efficient moderators of the positrons. The ORELA synchronized pulse starts the pulse sequence. Because of the negative work function of annealed tungsten for thermalized positrons, a usable fraction of the positrons are emitted at energies of 2–3 eV.

A -4-kV pulse supplied to the extraction tube accelerates the low-energy positrons to 4 keV. Then the 4-keV positrons bombard a tungsten film to produce low-energy positrons emitting from the rear face of the film. The time-of-flight distribution of the reemitted positrons has been measured and converted to the energy distribution which peaks at about 2.25 eV with a width of about 0.6 eV in FWHM (full width at half maximum). The second moderator can be biased either negatively or positively to control the positron kinetic energy in a range of 0–30 eV.

Positrons in the tube between the first moderator and the second moderator consist of two components in energy: (1) the accelerated 4-keV positrons, which produce tunable low-energy positrons after bombardment of the second moderator, as described above, and (2) fast positrons with energy between 10 and 120 keV. If these fast positrons pass through the second tungsten moderator, they will produce positrons with energies distributed from 5 eV to 100 keV. The resulting high energy cannot be controlled by the bias applied to the second moderator. Consequently, the resulting positrons are not characterized in energy. To avoid the fast-positron contribution, we used an about 50-G magnetic bending solenoid (200 cm in bending diameter) coupled with the bending tube. The bending coil with these conditions guides the positrons having energies below and about 4 keV to the second moderator, but not the fast positrons. If a higher magnetic field is applied in the bending tube, the fast positrons can be also guided with the mixture of 4-keV positrons. In fact, under the fast-positron mixture conditions, we observed water molecular ions from the H_2O residual gas even with -8 V applied to the remoderator. To ionize the water H_2O^+ by positronium formation, 6 eV energy is observed to be required. The production of the H_2O^+ ions with -8 V applied to the second moderator must be due to the fast-positron contribution. Thus we use H_2O^+ to monitor the presence of the fast posi-

trons. To be sure that our results are not due to the fast-positron contribution, we lower the bending coil current so that no H_2O^+ molecular ions are observed when we applied -8 V to the remoderator.

The Penning trap ionization volume, see Ref. [14], consists of input grid and output grid, spaced apart by ten cylindrically symmetric lenses. Two coils produce 1000 G of magnetic field in the center region of the trap. The trap is operated at a base pressure of 5.0×10^{-8} Torr. Vapors are admitted to the trap through a leak valve. Pressures range from 5.0×10^{-8} to 1.0×10^{-6} Torr. After introducing the low-energy positrons, the input grid returns to the constant positive bias. The positively biased input and output grids prevent longitudinal escape of the positrons and ions. The magnetic field prevents radial escape.

The Penning trap increases the collision path between positron and molecules, thereby enhancing the ionization counting rate. However, this apparatus makes the ionization volume large. Consequently, the large ion-containing volume would result in bad resolution in a conventional TOF spectrometer. To overcome the large ionization volume effect, a varying electrostatic field is used in which the potential varies as the square of the distance of the ion from the detector. This quadratic potential makes the flight times of ions of the same mass insensitive to their starting positions. The lenses of the trap are set to ground potential during the period when positrons are inside the trap. Following the positron-escape pulse, the lenses are pulsed to the quadratic-potential state. The accelerated ions are detected by a microchannel plate detector. Times of flight to the detector are recorded by a time-to-digital converter (TDC), interfaced through a computer-aided measurement-and-control (CAMAC) unit to a personal computer.

III. RESULTS

A. Butylbenzene

The fragmentation behavior of the gas-phase *n*-butylbenzene ($C_6H_5C_4H_9$) has been studied by other excitation processes [1–5]. The molecular ion (mass 134), plus fragment ions of mass 92 ($C_6H_5CH_3^+$) are produced when low internal energies are imparted by the ionization processes. Fragment ions of mass 91 ($C_6H_5CH_2^+$) are produced when higher internal energies are imparted by the ionization processes. Figure 2 shows time-of-flight mass spectra produced by positron impact on butylbenzene molecules as a function of incident positron energies. The Penning trap was filled with butylbenzene vapor at a pressure of 5.3×10^{-7} Torr. Two-hundred-thousand positron pulses are used for each spectrum. The retention time of positrons in the Penning trap is set at 600 μsec prior to collecting ions. The Ps-formation threshold for butylbenzene is 1.89 eV ($V_{IP}-6.8$ eV), where V_{IP} is the ionization potential. As shown in Fig. 2(a), when the positron energy was adjusted below the threshold at 1.6 eV, the degree of ionization was very low. The Fig. 2(b) spectrum, generated by positrons having 3.0 eV average kinetic energy, shows only molecular-ion formation. Figure 2(c) shows that when the positron energy was raised to 6.0 eV, 4.11 eV above the Ps threshold, fragment ions are produced.

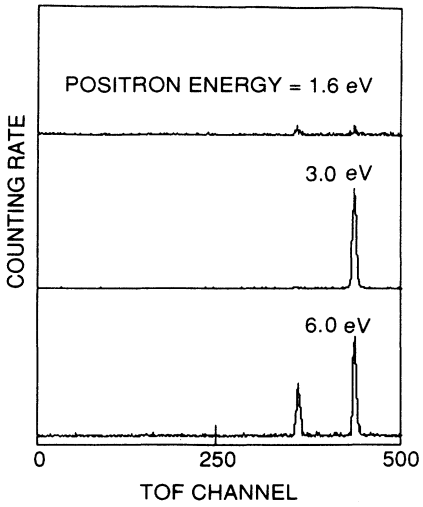

FIG. 2. Time-of-flight (TOF) mass spectra of butylbenzene as a function of positron energy.

Detailed energy dependence of the counting rates of molecular ions and fragment ions are shown in Fig. 3. The total yield is a summation of both molecular-ion and fragment-ion yields. In this plot, the positron energies

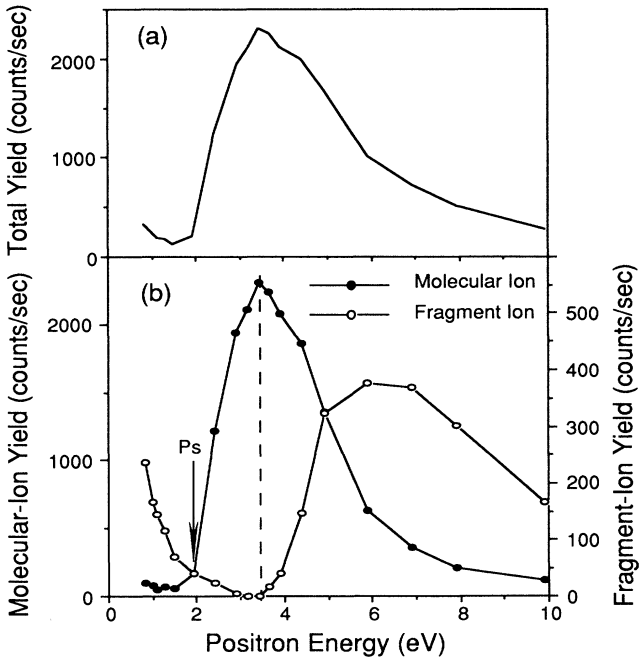

FIG. 3. Bottom: the yields of molecular ions (filled circle) and fragment ions (open circle) of butylbenzene as a function of positron energy. Upper: the summation of both the molecular-ion yield and the fragment-ion yield as a function of positron energy.

are weighted averages determined from the positron energy distribution. The ion yields are normalized to the incident positron flux. All yield curves in this paper have been treated in this way.

The total ion yield curve, as shown in Fig. 3(a), is consistent with the pattern of the cross sections for positronium formation, predicted by the Ore-gap model (reviewed in Ref. [15]). The Ore gap is defined as the energy range from the Ps threshold and the first excited-state energy. It is well documented [16,17] that the probability for positronium atom formation increases rapidly at the Ps threshold, and then stays approximately constant until its upper limit (first excitation energy) is reached. As the positron kinetic energy exceeds the higher edge of the Ore gap, the probability decreases and almost vanishes as the ionization potential of the molecule is approached. Except for the low-energy range (smaller than the Ps threshold), our measured total ionization yield as a function of incident positron energy correlated to the positronium-formation yield described by the Ore-gap model. The conclusion is that the ion production in the energy range from the Ps threshold to IP follows the positronium-formation process.

Our data reveal a pronounced difference between energy thresholds for molecular-ion production and for fragmentation, as shown in Fig. 3(b). Molecular ions are observed immediately as the positron kinetic energy reaches the Ps threshold, 1.89 eV, but fragment ions do not become prominent until the positron energy increases to 3.7 eV. This onset difference between the Ps threshold and the threshold for fragmentation is 1.85 eV. Later discussions will show that this onset difference is related to the dissociation energy required for the fragmentation. As shown by the dashed line in Fig. 3, increases in the fragment-ion populations in the mass spectra are accomplished by decreases in molecular-ion population.

It is seen that fragmentation of butylbenzene increases as the positron energy is lowered below 3 eV. The enhancement of fragmentation for positron energies at or below the Ps threshold was observed for all the molecules studied. The rapid removal of the electron from the molecule by positron annihilation is believed to be the cause of this effect. As will be discussed in more detail in Sec. IV C, the sudden removal of the electron is possibly due to either electron pickoff by the positron, or attachment of the positron to the molecule, followed by annihilation.

B. Decane

Figure 4(a) shows the mass spectrum of decane ($C_{10}H_{22}$), taken with an average positron energy of 7 eV, which is above the Ps-formation threshold for this molecule. The Penning trap was filled with decane vapor at a pressure of 1.1×10^{-6} Torr. Spectra were recorded for retention times varying from 50 to 1800 μsec. The absolute intensities of the ions increased to a maximum for a retention time of 600 μsec, but the relative distributions of the fragment ions changed only slightly. This is evidence that charge exchange or other secondary processes are not involved in the ionization. The spectra for Figs. 4(a) and 4(b) were recorded using retention times of 400

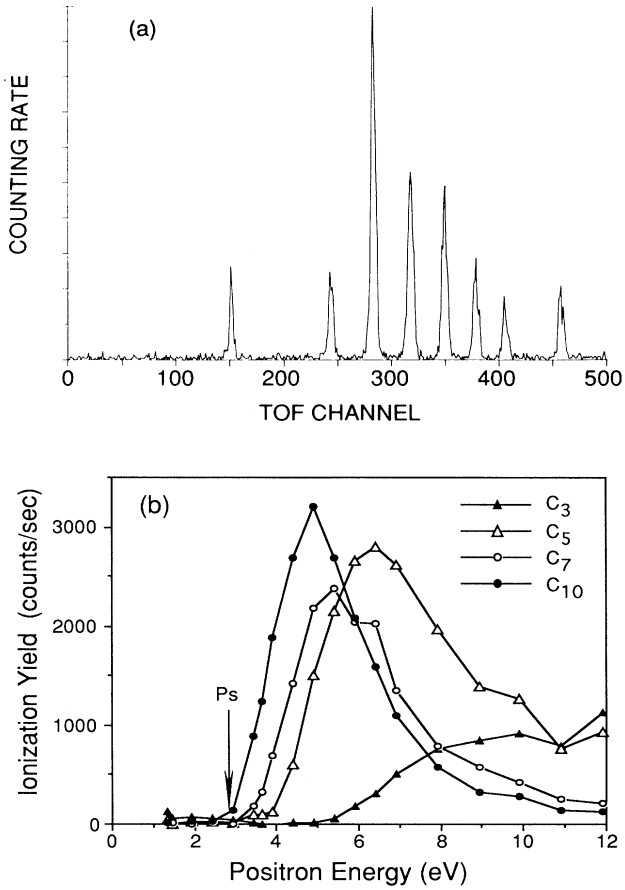

FIG. 4. (a) TOF mass spectrum of decane under 7-eV positron impact. (b) Ionization yields of decane as a function of positron energy.

μsec. The water peak shown in Fig. 4(a) was generated from background vapor in the system. The 7-eV positrons were sufficiently high in energy to ionize water by the Ps-formation mechanism.

Figure 4(b) shows positron energy dependence of the C_3, C_5, and C_7 fragment ions, and the C_{10} molecular ion. The C_4, C_6, and C_8 fragment ions showed similar patterns. The positronium threshold for decane is 2.85 eV ($V_{IP}-6.8$ eV), where V_{IP} is the ionization potential. Similarly to butylbenzene, the decane molecular ions were produced at about the Ps threshold energy. Fragment-ion intensities were lower than those of the molecular ion for positron energies below 4 eV. The data show an inverse relationship between the size of the ion fragments and the excess positron energy, above the Ps threshold, required to form them. For C_8, C_7, C_6, C_5, and C_3 fragment ions, they are 0.3, 0.45, 0.6, 1.1, and 2.4 eV, respectively. The C_4 ion, with an onset energy of 0.7 eV above the Ps threshold, is an exception. It is seen from Fig. 4(b) that the energies for which the populations of the different fragment ions reach maxima also bear an inverse relation to fragment size.

C. Tetraethylsilane and other molecules

Figure 5(a) shows the time-of-flight mass spectrum for tetraethylsilane [$(C_2H_5)_4Si$] for a positron energy of 4.5 eV, which is 2.4 eV above the Ps-formation threshold for this molecule. The four peaks of largest intensity are due to the molecular ion, $SiEt_4$, and the fragments $SiEt_3$, $SiEt_2$, and $SiEt_1$, arising from the successive losses of ethyl groups (Et). The small intermediate peaks are due to losses of methyl groups. Spectra for tetraethylsilane were measured as a function of Penning trap retention time. Similar to the decane results, the total ion yields, as a function of retention time, were found to go through maxima, but the relative intensities of the molecular ion and the fragment ions did not change appreciably. The retention time for Fig. 5(a) was 400 μsec.

Figure 5(b) shows positron energy dependence of the intensities of $SiEt_1$, $SiEt_2$, and $SiEt_3$ fragment ions and the $SiEt_4$ molecular ion. The positronium threshold for tetraethylsilane is 2.1 eV ($V_{IP}-6.8$ eV). For this molecule also, is seen that molecular ions are produced at the Ps threshold energy. The data show that onset energies for $SiEt_3$, $SiEt_2$, and $SiEt_1$ fragments are 0.10, 1.9, and 3.9 eV, respectively. The $SiEt_1$ onset energy could not be accurately measured because of low counting rates for this ion and the large energy step used. The results for positron ionization of tetraethylsilane are consistent with those observed for decane and butylbenzene. Smaller fragment ions require higher onset energies than larger fragment ions. Later discussion will show that this onset is related to the dissociation energy required for the fragmentation.

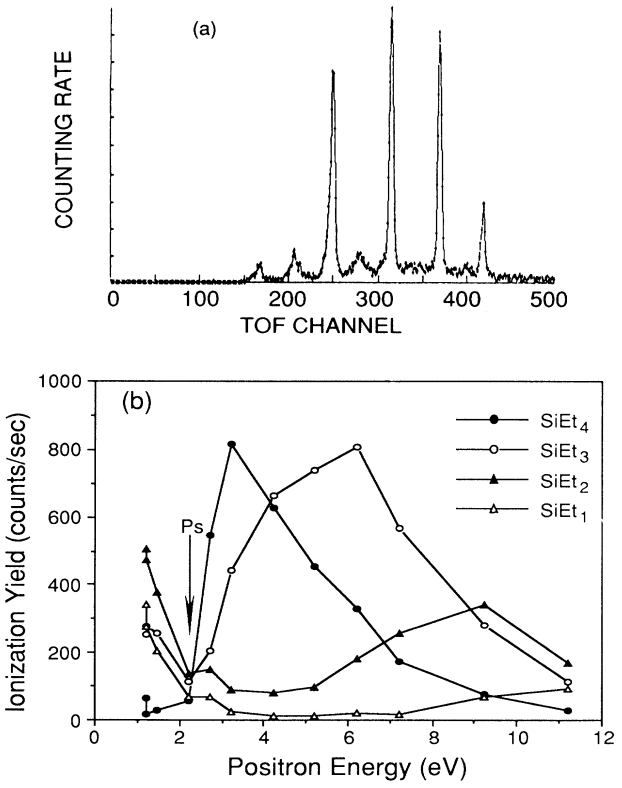

FIG. 5. (a) TOF mass spectrum of tetraethylsilane under 4.5-eV positron impact. (b) The ionization yield as a function of positron energy.

The ionization of benzene by interaction with positrons was also observed. For energies in the range of 2–10 eV, large amounts of molecular ion were produced; no fragmentation occurred. The absence of fragmentation is probably due to the very large amount of energy, 5.8 eV, required for dissociation. To produce fragment ions, the positrons must have energies of about 8 eV, which is greater than the first excited state for benzene. For positrons with energies this high, the positron-molecule interactions occur through another channel, in which molecular excitation occurs instead of ionization.

Qualitative results for dodecane, octane, and hexene indicate that in these cases also smaller fragment ions require higher onset energies than larger fragment ions.

IV. DISCUSSION

A. Correlation of fragmentation threshold to dissociation energy

For the molecules studied above, the energy requirements for ionization and fragmentation by positronium formation appear to parallel those for other means of ionization. Ionization-potential studies show that for ionization by electrons and photons a minimum amount of energy is required for removing one electron and producing a molecular ion. If sufficient energy, in excess of this minimum, is imparted to the molecule, fragmentation can occur. The magnitudes of these energies have been measured and tabulated as critical dissociation energies, i.e., the summation of the enthalpies of formation of the fragment ion and the fragment neutral minus the enthalpy of formation of the molecular ion [18]. The results of our studies show that if the kinetic energy with which the positron impacts the molecule plus the 6.8 eV imparted to the molecule by positronium formation is equal to the ionization potential of the molecule, the molecular ion is formed. The intensities of ion fragments for spectra generated at the positronium thresholds are usually very low or not measurable. If the bombarding positrons are given kinetic energies sufficiently in excess of the positronium threshold, fragmentation will occur.

We have designated the difference between the positron kinetic energy required for an ion fragment appearance and the positronium threshold as the "onset energy" for that ion. For a large number of cases the positron onset energies for ion fragmentation have been measured to be equal to their tabulated critical dissociation energies. Figure 6 shows a plot of the measured onset energies of the fragment ions as a function of the corresponding dissociation enthalpies for the assigned reactions in Table I. It is seen from Fig. 6 and Table I [18] that the measured onset energies correlate to the dissociation energies.

The onset energy for the C_4 fragments is lower than that calculated, and can be accounted for: $C_4H_9^+$ can be produced by secondary processes. For example, if

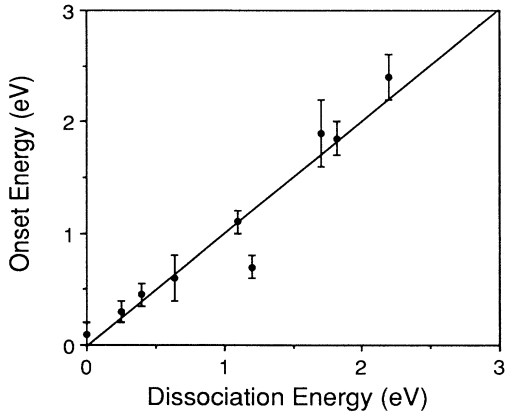

FIG. 6. The measured onset energies for fragment ions as a function of the corresponding dissociation energies.

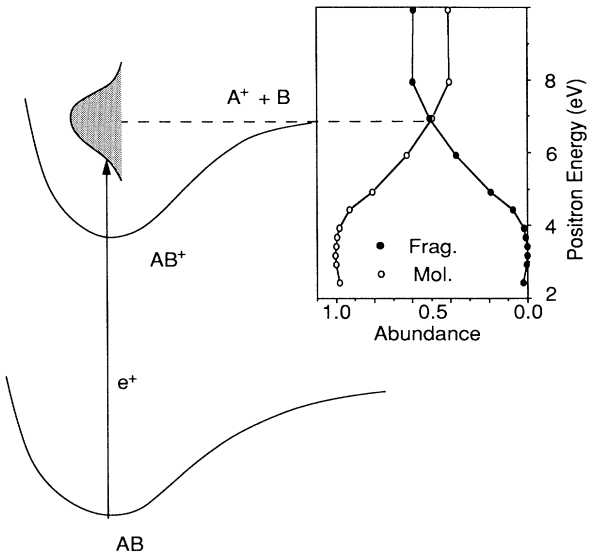

FIG. 7. The proposed process responsible for positron-induced ionization and fragmentation under positronium-formation conditions. Upper-right corner: The crossover diagram for the molecular ion and the fragment ion of butylbenzene as a function of positron energy.

$C_7H_{15}^+$ is generated with sufficient energy from decane it can further fragment into $C_4H_9^+$ and C_3H_6. The energetics of $C_3H_7^+$ ion formation from $C_7H_{15}^+$ ions are not favorable. Secondary processes such as this may explain the spectral dominance of the C_4 ion and its lower onset energy. Other ions may have similar secondary formation paths, but theirs are apparently not as prominent as those for the C_4 fragment ion.

B. Mechanism for positron-induced dissociative ionization

We proposed a two-step mechanism for ionization and fragmentation under conditions of positronium formation. The proposed mechanism is shown in a potential energy diagram scheme in Fig. 7 and written in the equations below:

$$e^+ + M \rightarrow M^{+*} + \mathrm{Ps}\ , \tag{1}$$

$$M^{+*} \rightarrow m_1^+ + m_2\ . \tag{2}$$

In this mechanism two processes are involved. First, the positron, having kinetic energy $E_{\mathrm{kin}}(e^+)$, strips an electron from the molecule to form the positronium atom and the molecular ion. The excess energy of the reaction (in eV) is $E_{\mathrm{kin}}(e^+)-(V_{\mathrm{IP}}-6.8\ \mathrm{eV})$. This excess energy is partitioned between the kinetic energy of the positronium atom and internal energy of the molecular ion. If the molecular ion has sufficient internal energy it will undergo unimolecular decay to form a fragment ion and a neutral fragment.

TABLE I. The dissociation energies and the measured onset energies above the positronium-formation thresholds for the fragmentation reactions.

Fragmentation reaction	Dissociation energy (eV)	Measured onset energy (eV)
$C_{10}H_{14}^+ \rightarrow C_7H_8^+ + C_3H_6^{\cdot}$	1.82	1.85±0.15
$C_8H_{20}Si^+ \rightarrow C_6H_{14}Si^+ + C_2H_6^{\cdot}$	0.0	0.1±0.1
$C_8H_{20}Si^+ \rightarrow C_4H_{12}Si^+ + C_4H_8^{\cdot}$	1.7	1.9±0.3
$C_8H_{20}Si^+ \rightarrow C_2H_6Si^+ + C_6H_{14}^{\cdot}$	2.24	3.9±2.0
$C_{10}H_{22}^+ \rightarrow C_8H_{17}^+ + C_2H_5^{\cdot}$	0.25	0.3±0.1
$C_{10}H_{22}^+ \rightarrow C_7H_{15}^+ + C_3H_7^{\cdot}$	0.4	0.45±0.10
$C_{10}H_{22}^+ \rightarrow C_6H_{13}^+ + C_4H_9^{\cdot}$	0.64	0.6±0.2
$C_{10}H_{22}^+ \rightarrow C_5H_{11}^+ + C_5H_{11}^{\cdot}$	1.1	1.1±0.1
$C_{10}H_{22}^+ \rightarrow C_4H_9^+ + C_6H_{13}^{\cdot}$	1.2	0.7±0.1
$C_{10}H_{22}^+ \rightarrow C_3H_7^+ + C_5H_{15}^{\cdot}$	2.2	2.4±0.1

The features expected from this mechanism are consistent with the experimental data. In the upper right-hand corner of Fig. 7 is a plot of the fractional abundance of the molecular ion and fragment ions of butylbenzene as a function of the positron energy. At positron energies near the Ps threshold, there is not enough excess energy in the reaction to cause the molecular ion to dissociate. Therefore the relative molecular-ion abundance is unity. At higher positron energies, there is sufficient excess energy in the reaction, which can be partitioned into internal energy of the molecular ion, to overcome the dissociation barriers. Fragment ions begin to be formed when the kinetic energy of the positron exceeds the positronium threshold by 1.8 eV, which is the critical energy for dissociation of butylbenzene.

The slope of the crossover curve represents the internal energy distribution in this model. Even in a case in which there are only monoenergetic positrons, a range of internal energies will result due to the partitioning of energy between internal energy and kinetic energy of positronium. With a distribution of positron kinetic energies, an even broader distribution of internal energies is expected. This is observed in the data presented in Fig. 7 where a 0.6-eV energy distribution of positrons (FWHM) produced almost a 4-eV range over which the fragmentation increases.

Another possible mechanism is the formation of the exotic compound proposed by Schrader [19] for diatomic fragmentation. This mechanism is written below:

$$e^+ + AB \rightarrow A^+ + \mathrm{Ps}\,B \ . \quad (3)$$

In this model, the resulting positronium attaches to a neutral fragment and a fragment ion is directly produced in the one-step process. Schrader's model predicts that the onset energy for the fragmentation is smaller than the unimolecular dissociation energy of the molecular ion. Recent measurements [20] indicate that the formation of PsH lowers the threshold energy for generating the CH_3^+ fragment from methane. However, in our work, the correlation between the unimolecular dissociation energy and the measured onset energy supports the stripping mechanism followed by unimolecular dissociation of the molecular ion.

C. Subpositronium dissociative ionization

The data discussed above were generated by positrons having energies above the Ps threshold. Many studies have also been done in the "subpositronium" range, in which the positron energies were below the positronium-formation threshold. We plan to give the details in a separate publication [21]. Below the Ps threshold the ion fragmentation patterns change dramatically, in that the intensities of the molecular ions become either very low or unmeasurable, and the fragment ions dominate. As shown graphically in Fig. 3 for butylbenzene, and in Fig. 5 for tetraethylsilane, the counting rate of fragment ions for subpositronium conditions is observed to increase as the positron kinetic energy decreases.

We conclude that ionization processes under subpositronium conditions proceed by mechanisms totally different from those of the positronium-formation process. Either electron pickoff or positron attachment is involved. Adapting the Dirac cross-section equation for electron pickoff by positrons moving in a free-electron gas to the case for annihilation of electrons on molecules [22], we have

$$\sigma = 5\times 10^{-22} Z(\mathrm{eff})/E^{1/2} \quad (4)$$

where $Z(\mathrm{eff})$ is the effective atomic number, and E is the kinetic energy of the positron.

The number of ions produced in the Penning trap is proportional to the above cross section multiplied by the positron velocity, which is directly proportional to $E^{1/2}$. Since the observed ionization counting rate increases as the positron energy decreases, we must argue that $Z(\mathrm{eff})$ is a function of positron energy in order to ascribe the subpositronium ionization processes to electron pickoff. The positron attachment mechanism described by Surko and co-workers [12] is an alternative explanation for subpositronium ionization. Our data are not sufficient to distinguish between the electron pickoff and attachment mechanisms.

V. CONCLUSIONS

We have measured positron ionization time-of-flight mass spectra of butylbenzene, decane, tetraethylsilane, and other organic molecules as functions of positron kinetic energies. It has been found that, in contrast to molecular-ion production, which in general follows the positronium formation, fragment ions are produced with the following features.

(1) An additional onset energy above the Ps threshold is required to produce fragment ions.

(2) The onset energy depends on the nature of the fragment ions and correlates to the dissociation energy of the corresponding reaction initiated from the molecular ions.

(3) As the probability for fragmentation increases, that for molecular-ion production decreases.

Based on these observations, we propose that fragmentation by positronium formation occurs by a two-step process: (1) An electron is stripped from the molecule to form a positronium atom and molecular ion, and (2) Excess energy imparted to the molecular ion remaining from step 1 causes it to undergo unimolecular dissociation to smaller fragments. Our results indicate that the degree of dissociation can be controlled by selecting positron incident energy and that positron-induced dissociation offers another technique for molecular studies and for investigation of positron-matter interaction.

ACKNOWLEDGMENTS

We thank R. W. Shaw of Oak Ridge National Laboratory, D. M. Schrader of Marquette University, and C. M. Surko of the University of California, San Diego, for their helpful comments. We also thank the staff of Oak Ridge Electron Linear Accelerator (ORELA) for their helpful support.

*Present address: Department of Chemistry, University of North Carolina, Chapel Hill, NC 27599.

[1] K.-M. Weitzel, J. A. Booze, and T. Baer, Chem. Phys. **150**, 263 (1991).

[2] J. H. Chen, J. D. Hays, and R. C. Dunbar, J. Phys. Chem. **88**, 4759 (1984).

[3] S. Nacson and A. G. Harrison, Int. J. Mass Spectrom. Ion Processes **63**, 325 (1985).

[4] J. H. Futrell and T. O. Tiernan, J. Chem. Phys. **39**, 2539 (1963).

[5] R. B. Cody and B. S. Freiser, Anal. Chem. **59**, 1054 (1987).

[6] M. W. Karl, H. Nakanishi, and D. M. Schrader, Phys. Rev. A **30**, 1624 (1984).

[7] D. L. Donohue, L. D. Hulett, Jr., B. A. Eckenrode, S. A. McLuckey, and G. L. Glish, Chem. Phys. Lett. **168**, 37 (1990).

[8] S. A. McLuckey, G. L. Glish, D. L. Donohue, and L. D. Hulett, Jr. Int. J. Mass Spectrom. Ion Processes **97**, 237 (1990).

[9] A. Passner, C.M. Surko, M. Leventhal, and A. P. Mills, Jr., Phys. Rev. A **39**, 3706 (1989).

[10] M. S. Dobobneh, Y.-F. Hsieh, W. E. Kauppila, C. K.

Kwan, S. J. Smith, T. S. Stein, and M. N. Uddin, Phys. Rev. A **38**, 1207 (1988).
[11] D. M. Schrader and C. M. Wang, J. Phys. Chem. **80**, 2507 (1976).
[12] C. M. Surko, A. Passner, M. Levinthal, and F. J. Wysocki, Phys. Rev. Lett. **61**, 1831 (1988).
[13] D. L. Donohue, L. D. Hulett, S. A. McLuckey, G. L. Glish, and H. S. McKown, Int. J. Mass Spectrom. Ion Processes **97**, 227 (1990).
[14] Lester D. Hulett, David L. Donohue, and T. A. Lewis, Rev. Sci. Instrum. **62**, 2131 (1991).
[15] D. M. Schrader and R. E. Svetic, Can. J. Phys. **60**, 517 (1982).
[16] R. N. West, Adv. Phys. **22**, 263 (1973); V. I. Godlanskii, At. Energy Rev. **6**, 3 (1968).
[17] M. Charlton, T. C. Griffith, G. R. Hayland, K. S. Lines, and G. L. Wright, J. Phys. B. **13**, L757 (1980).
[18] S. Lias, J. E. Bartmess, J. F. Fiebman, J. L. Holmes, R. D. Levin, and W. G. Mallard, J. Phys. Chem. Ref. Data **17**, Suppl. 1 (1988).
[19] D. M. Schrader, in *The 8th International Conference on Positron Annihilation,* edited by L. Dorikens-Vanpraet, M. Dorikens, and D. Seers (World Scientific, Singapore, 1988), p. 609.
[20] D. M. Schrader, T. Yoshida, and K. Iguchi, Phys. Rev. Lett. **68**, 3281 (1992).
[21] Lester Hulett, Jr., David Donohue, Jun Xu, T. A. Lewis, Scott McLuckey, and Gary Glish (unpublished).
[22] P. A. M. Dirac, Proc. Cambridge Philos. Soc. **26**, 361 (1930).